

On the Measurement of Solar Neutrino Oscillation Parameters with KamLAND

Abhijit Bandyopadhyay¹, Sandhya Choubey^{2,3}, Srubabati Goswami⁴, and S.T. Petcov^{3,2,5}

¹*Saha Institute of Nuclear Physics, 1/AF, Bidhannagar, Calcutta 700 064, INDIA*

²*INFN, Sezione di Trieste, Trieste, Italy*

³*Scuola Internazionale Superiore di Studi Avanzati, I-34014 Trieste, Italy*

⁴*Harish-Chandra Research Institute, Chhatnag Road, Jhusi, Allahabad 211 019, INDIA and*

⁵*Institute of Nuclear Research and Nuclear Energy,
 Bulgarian Academy of Sciences, 1784 Sofia, Bulgaria*

A new reactor power plant Shika-2, with a power of approximately 4 GW and at a distance of about 88 km from the KamLAND detector is scheduled to start operating in March 2006. We study the impact of the $\bar{\nu}_e$ flux from this reactor on the sensitivity of the KamLAND experiment to the solar neutrino oscillation parameters. We present results on prospective determination of Δm_{\odot}^2 and $\sin^2 \theta_{\odot}$ using the combined data from KamLAND and the solar neutrino experiments, including the effect of the Shika-2 contribution to the KamLAND signal and the latest data from the salt enriched phase of the SNO experiment. We find that contrary to the expectations, the addition of the Shika-2 reactor flux does not improve the $\sin^2 \theta_{\odot}$ sensitivity of KamLAND, while the ambiguity in Δm_{\odot}^2 measurement may even increase, as a result of the averaging effect between Kashiwazaki and the Shika-2 reactor contributions to the KamLAND signal.

PACS numbers: 14.60.Pq 13.15.+g

I. INTRODUCTION

There has been a significant progress in the studies of neutrino oscillations in the last two years. The evidences for solar neutrino oscillations/transitions, obtained in the solar neutrino experiments Homestake, Kamiokande, SAGE, GALLEX/GNO, Super-Kamiokande (SK) [1, 2] were reinforced by the first data of the SNO experiment [3] on the charged current (CC) reaction induced by solar neutrinos, $\nu_e + D \rightarrow e^- + p + p$. When combined with the data from the Super-Kamiokande experiment [2], the SNO results clearly demonstrate the presence of $\nu_{\mu,\tau}$ and/or $\bar{\nu}_{\mu,\tau}$ component in the flux of solar neutrinos reaching the Earth. This compelling evidence for oscillations and/or transitions of the solar neutrinos was further strengthened in 2002 by the SNO results [4], including the data on the neutral current (NC) reaction $\nu + D \rightarrow \nu + n + p$ due to solar neutrinos. In 2002 the first data from the KamLAND experiment were published [5]. The KamLAND results represent the first strong evidence (more than 3σ effect) for neutrino oscillations obtained in an experiment with terrestrial neutrinos. Under the assumption of CPT-invariance, the KamLAND data practically establish [5] the large mixing angle (LMA) MSW solution as unique solution of the solar neutrino problem. All other mechanisms which could cause transitions of the solar ν_e into $\nu_{\mu,\tau}$ and/or $\bar{\nu}_{\mu,\tau}$ and which were considered as possible solutions of the solar neutrino ‘‘puzzle’’, such as VO, SMA MSW, QVO, LOW (see, e.g., [6]), RSFP [7], FCNC [8], WEPV and LIV [9], if not completely ruled out, are constrained by the KamLAND data to play at most a sub-dominant secondary role in the physics of the solar neutrino transitions. This result brings us, after more than 30 years of research, initiated by the pioneering works of B. Pontecorvo [10] and the experiment of R. Davis et al. [11], very close to a complete understanding of the true cause of the solar neutrino problem.

The combined two-neutrino oscillation analyses of the available solar neutrino and KamLAND data identified two distinct solution sub-regions within the LMA solution region (see, e.g., [12, 13]). The best fit values of the two-neutrino oscillation parameters - the solar neutrino mixing angle θ_{\odot} and the neutrino mass squared difference Δm_{\odot}^2 , in the two sub-regions - low-LMA and high-LMA, were given respectively by [12]: $\Delta m_{\odot}^2 = 7.2 \times 10^{-5} \text{ eV}^2$, $\sin^2 \theta_{\odot} = 0.3$ $\Delta m_{\odot}^2 = 1.5 \times 10^{-4} \text{ eV}^2$, $\sin^2 \theta_{\odot} = 0.3$ The low-LMA solution was statistically preferred by the data. At 99.73% C.L. the two solutions merged and the allowed ranges were [12]:

$$\Delta m_{\odot}^2 \cong (5.0 - 20.0) \times 10^{-5} \text{ eV}^2, \quad \sin^2 \theta_{\odot} \cong (0.21 - 0.47) . \quad (1)$$

Very recently the SNO collaboration published the data from the salt phase of the experiment [14]. Addition of

NaCl in the heavy water increases the efficiency of capture for the final state neutrons of the NC reaction resulting in a gamma ray cascade with a peak around 8 MeV. This, apart from increasing the statistics of the NC data allowed the SNO collaboration to report the CC and NC total event rates with a higher precision and without the assumption of an undistorted energy spectrum. For the ratio of the CC and NC event rates, in particular, the collaboration finds: $R_{CC/NC} = 0.306 \pm 0.026 \pm 0.024$. Adding the statistical and the systematic errors in quadratures one gets at 99.73% C.L.: $R_{CC/NC} \leq 0.41$. As was shown in [15], an upper limit of $R_{CC/NC} < 0.5$ implies a significant upper limit on Δm_{\odot}^2 smaller than $2 \times 10^{-4} \text{ eV}^2$. Thus, the new SNO data on $R_{CC/NC}$ implies stringent constraints on the high-LMA solution. A combined analysis of the data from the solar neutrino and KamLAND experiments, including the latest SNO results, shows [16, 17] that the high-LMA solution is allowed only at 99.73% C.L. and restricts the 3σ allowed upper limit of Δm_{\odot}^2 to $\Delta m_{\odot}^2 < 1.7 \times 10^{-4} \text{ eV}^2$.

There exists also very strong evidences for oscillations of the atmospheric ν_{μ} ($\bar{\nu}_{\mu}$) from the observed Zenith angle dependence of the multi-GeV μ -like events in the SK experiment [18]. The Super-Kamiokande (SK) atmospheric neutrino data is best described in terms of dominant $\nu_{\mu} \rightarrow \nu_{\tau}$ ($\bar{\nu}_{\mu} \rightarrow \bar{\nu}_{\tau}$) oscillations with maximal mixing and $1.3 \times 10^{-3} \text{ eV}^2 \lesssim |\Delta m_{\text{A}}^2| \lesssim 3.1 \times 10^{-3} \text{ eV}^2$ (90% C.L.), where we have quoted the preliminary results of an improved analysis of the SK atmospheric neutrino data, performed recently by the SK collaboration [19].

After these remarkable developments in the field of neutrino oscillations, further progress in the studies of neutrino mixing requires the realization of large and challenging program of research in neutrino physics (see, e.g., [20]). As one of its main goals we see higher precision determination of the neutrino mass and mixing parameters which control the solar neutrino oscillations, Δm_{\odot}^2 and θ_{\odot} . With the future data from SNO on the day-night effect and the spectrum of e^{-} from the CC reaction, and the future high statistics data from KamLAND, one can look forward, in particular, to resolving completely the low-LMA - high-LMA solution ambiguity, and at the same time constraining the solar neutrino mixing angle [12, 15, 21, 22, 23].

In general, the solar neutrino oscillations parameters Δm_{\odot}^2 and $\sin^2 \theta_{\odot}$ can be measured either in solar neutrino experiments, or in long baseline reactor antineutrino experiments. The potential of the current and future solar neutrino experiments for precision measurements of Δm_{\odot}^2 and $\sin^2 \theta_{\odot}$ was studied in detail recently in [24, 25]. The just published high statistics NC data from SNO together with the earlier SNO data constrain the mixing angle $\sin^2 \theta_{\odot}$ from above: the case of maximal mixing is excluded by these data at more than 5 s.d. The data from the proposed low energy experiments sensitive to the pp neutrinos could help constrain $\sin^2 \theta_{\odot}$ from below, provided the total error in these experiments could be reduced to $\lesssim 1\%$ [24, 25]. The recent SNO salt data has also disfavoured higher values of Δm^2 and the high-LMA region is shown to be allowed only at 3σ [16, 17]. In [16] it is shown that with 1 kTy statistics the KamLAND data can further narrow down the high-LMA allowed zone if the true KamLAND spectrum corresponds to values of Δm^2 in the low-LMA region. However, if the observed KamLAND spectrum corresponds to high-LMA solution, the low-LMA/high-LMA ambiguity would increase as a result of conflicting trends of solar and KamLAND data.

Precision measurements of the solar neutrino oscillation parameters can be performed in reactor $\bar{\nu}_e$ experiments sensitive to the modulation of the antineutrino spectrum caused by the Δm_{\odot}^2 -driven oscillations in vacuum. The possibility to observe such a modulation depends crucially on the chosen baseline. When the baseline corresponds to $\sin^2(\Delta m_{\odot}^2 L/E) \approx 1$, the neutrinos undergo maximum flavor transition and in this case the survival probability $P_{ee} \approx 1 - \sin^2 2\theta_{\odot}$ is in its minimum. We will use the term Survival Probability MINima (SPMIN) to denote such a case. If the baseline corresponds to $\sin^2(\Delta m_{\odot}^2 L/E) \approx 0$, one has $P_{ee} \approx 1$ and we will refer to this case as Survival Probability MAXima (SPMAX). While for a given reactor experiment both conditions depend crucially on Δm_{\odot}^2 , in the case of the SPMAX condition there is no θ_{\odot} -dependence. Thus, while Δm_{\odot}^2 can be determined with a relatively good precision in an experiment sensitive to either SPMAX or SPMIN, for achieving a relatively precise measurement of the mixing angle θ_{\odot} the baseline should be tuned to SPMIN.

All studies of the potential of KamLAND to measure the solar neutrino oscillation parameters [12, 22, 23, 24], have shown that the KamLAND experiment has a remarkable sensitivity to Δm_{\odot}^2 . Its expected sensitivity to $\sin^2 \theta_{\odot}$ was not found to be equally good [24]. Even with 3 kTy statistics and extremely optimistic systematic error of only 3%, the constraints on $\sin^2 \theta_{\odot}$ were found to be not much better than that obtained using the solar neutrino data (see [24] for a detailed discussion). The reason for this can be traced to the fact that effectively the baseline relevant in the KamLAND experiment corresponds to SPMAX for both the low-LMA and high-LMA solutions.

In [24] a 70 km baseline reactor $\bar{\nu}_e$ experiment was proposed, to measure with high precision the solar neutrino oscillation parameters in the case of the low-LMA solution. If high-LMA happens to be the true solution – a possibility which is strongly disfavored by the current data – an intermediate baseline reactor experiment with $L = 20 \div 30$ km would be needed for the purpose [26, 27]. Such an experiment would not only allow measurement of Δm_{\odot}^2 and $\sin^2 \theta_{\odot}$ with high precision, but could also constrain $\sin^2 \theta$ and Δm_{A}^2 [27]. Under rather demanding conditions, the same experiment could provide information on the neutrino mass hierarchy [26, 27].

Both proposals for new reactor experiments discussed briefly above were made after detailed studies of the

KamLAND physics potential in which prolonged periods of data taking were assumed. However, there are new upcoming reactor power plants relatively close to KamLAND. Their presence may affect the conclusions reached in these studies. More concretely, there are plans to build a new reactor, Shika-2, very close to the site of the existing reactor Shika-1, which is located at about 88 km from KamLAND [28]. The new reactor is expected to have a power of approximately 3.926 GW and is due to start operations in March of 2006. In this paper we study the impact the flux of $\bar{\nu}_e$ from the new Shika-2 reactor can have on the sensitivity of the KamLAND experiment to the solar neutrino oscillation parameters. We present our results for the KamLAND detector before and after the starting of the new reactor power plant. Finally we do a global analysis of solar and KamLAND data in our analysis including the effect of the Shika-2 contribution to the KamLAND signal and the just published salt data from the SNO experiment.

II. THE $\bar{\nu}_e$ SURVIVAL PROBABILITY AT KAMLAND

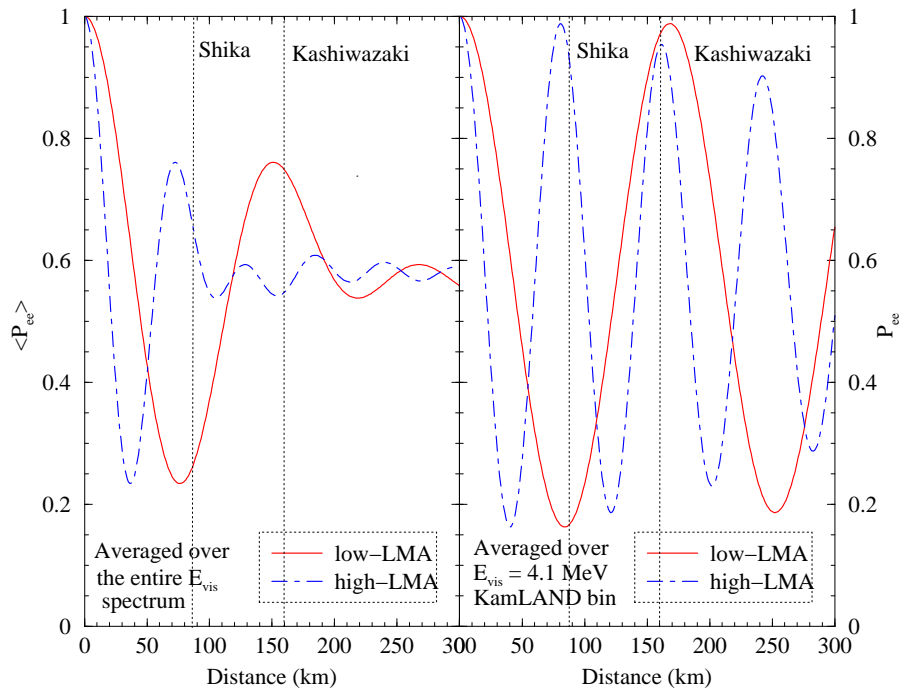


FIG. 1: The predicted suppression of the event rate in the KamLAND experiment in the cases of low-LMA (solid line) and high-LMA (dashed line) solutions, as a function of the baseline L . The left-hand panel shows the probability averaged over the entire positron energy spectrum. The right-hand panel shows the survival probability averaged over the bin with central energy of $E_{vis} = 4.1$ MeV and width of 0.425 MeV. Also marked are the distances of the Kashiwazaki and Shika reactor power plants from KamLAND.

The $\bar{\nu}_e$ flux at KamLAND detector receives contributions from a large number of nuclear power plants located in different parts of Japan and in South Korea. The most powerful is the Kashiwazaki reactor complex, which has a total thermal power of 24.6 GW and is situated at a distance of about 160 km from KamLAND. A new reactor power plant, Shika-2, is being built a few hundred meters from the site of the existing Shika-1 reactor, which is located at about 87.7 km from KamLAND. The thermal power of the new Shika-2 reactor is about 3.926 GW. We take the distance from Shika-2 to KamLAND to be 87.7 km. It is expected that the Shika-2 plant will start commercial operation in March of 2006. Test operation will start several months before the commercial operation. In this Section we take into account the flux from the new Shika-2 reactor and find its impact on the sensitivity of KamLAND experiment to the solar neutrino oscillation parameters $\sin^2 \theta_\odot$ and Δm_\odot^2 .

The $\bar{\nu}_e$ flux from the various reactors in Japan (and South Korea) are detected in the KamLAND experiment through the inverse beta decay process $\bar{\nu}_e + p \rightarrow e^+ + n$. The number of events observed in the KamLAND detector

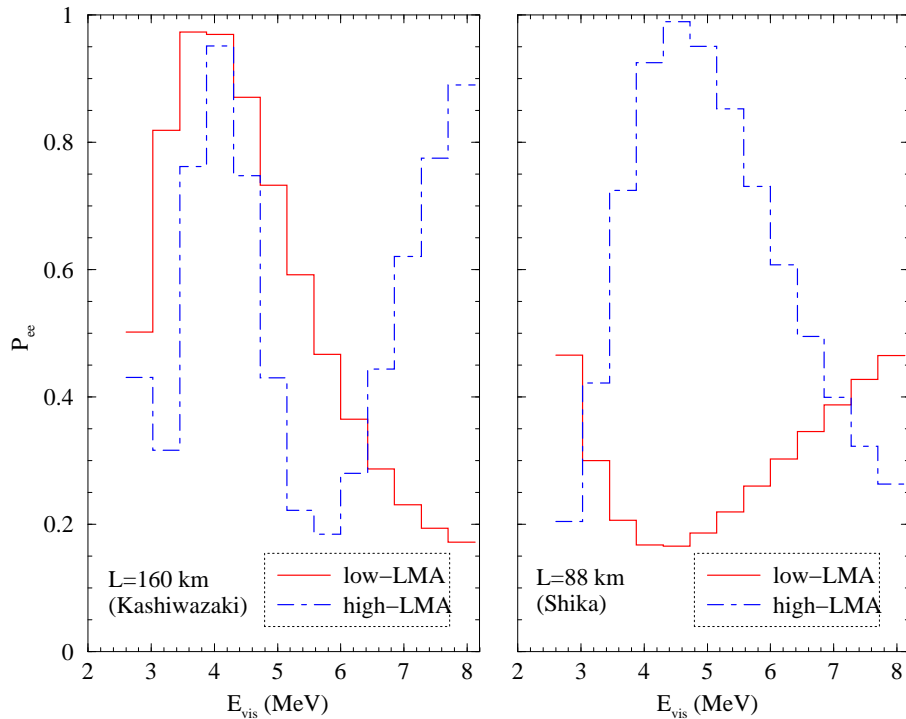


FIG. 2: The spectral distortion for the low-LMA (solid line) and high-LMA (dashed line) solutions, predicted to be observed in the KamLAND experiment if the flux of $\bar{\nu}_e$ was produced by i) the Kashiwazaki reactor complex (right-hand panel) and ii) the Shika-2 reactor (left-hand panel).

is given by

$$N_{KL} = N_p \int dE_{vis} \int dE_\nu \sigma(E_\nu) R(E_{vis}, E_\nu) \sum_i \frac{S_i(E_\nu)}{4\pi L_i^2} P_i(\bar{\nu}_e \rightarrow \bar{\nu}_e) \quad (2)$$

where E_{vis} is the measured *visible* energy of the emitted positron, when the true visible energy, $E_{vis}^T \cong E_\nu - 0.80$ MeV, E_ν being the energy of the incoming $\bar{\nu}_e$, $\sigma(E_\nu)$ is the $\bar{\nu}_e + p \rightarrow e^+ + n$ reaction cross-section, $S_i(E_\nu)$ denotes the $\bar{\nu}_e$ flux from the i th reactor, L_i is the distance between the i th reactor and KamLAND, $R(E_{vis}, E_\nu)$ is the energy resolution function of the detector, N_p are the number of protons in the target, and $P_i(\bar{\nu}_e \rightarrow \bar{\nu}_e)$ is the survival probability of the $\bar{\nu}_e$ coming from the reactor i . For the energy resolution we use $\sigma(E)/E = 7.5\%/\sqrt{E}$, as reported by the KamLAND collaboration [5]. We have used for N_p the number provided in [5]. The fiducial mass of the detector was given as 408 tons. Since this may change in the future and the total statistics of the experiment depends on the mass of detector material (in ktons) and the time of exposure (years), we choose the unit kton-year (kTy) to characterize the KamLAND statistics.

Apart from the solar neutrino oscillation parameters, the $\bar{\nu}_e$ survival probability $P_i(\bar{\nu}_e \rightarrow \bar{\nu}_e)$ depends on the energy of the antineutrinos and the distance L_i between the i th reactor and KamLAND :

$$P_i(\bar{\nu}_e \rightarrow \bar{\nu}_e) = 1 - \sin^2 2\theta_\odot \sin^2 \left(\frac{\Delta m_\odot^2 L_i}{4E} \right) \quad (3)$$

where it is assumed that $\bar{\nu}_e$ take part in two-neutrino oscillations. The KamLAND collaboration presented their data in 13 E_{vis} bins of width of 0.425 MeV. To get the events in each of the KamLAND bins, we integrate Eq. (2) between $E_{vis} - 0.425/2$ to $E_{vis} + 0.425/2$.

In Figure 1 we show the effects of the survival probability $P_i(\bar{\nu}_e \rightarrow \bar{\nu}_e)$ on the KamLAND event rate as a function of distance. The left-hand panel shows the probability averaged over the entire visible energy spectrum, while the right-hand panel illustrates the depletion the KamLAND detector would observe in the bin with central energy $E_{vis} = 4.1$ MeV. Thus, while the left-hand panel shows the predicted suppression of the event rate as a function of the reactor

distance, the right-hand panel gives an idea of the behavior of the observed spectral shape with distance. The effects of $P_i(\bar{\nu}_e \rightarrow \bar{\nu}_e)$ are shown both for the now strongly preferred low-LMA ($\Delta m_\odot^2 = 7.2 \times 10^{-5} \text{ eV}^2$, $\sin^2 \theta_\odot = 0.3$) and for the high-LMA ($\Delta m_\odot^2 = 1.5 \times 10^{-4} \text{ eV}^2$, $\sin^2 \theta_\odot = 0.3$) solutions. Marked on the figure are also the approximate distances of the Kashiwazaki and the Shika reactor power plants from KamLAND. From the left-hand panel we note that the signal due to the $\bar{\nu}_e$ flux from Kashiwazaki complex is suppressed due to the oscillations by a factor of ~ 0.75 (0.54) for the low-LMA (high-LMA) solution. The signal due to $\bar{\nu}_e$ from the Shika reactor is reduced by a factor of ~ 0.26 (0.64) in the case of the the low-LMA (high-LMA) solution. The event rate observed in KamLAND with 162 ton-yr of data corresponds to 0.61 of the rate predicted in the absence of oscillations. This is the rate observed in the detector taking into account the contributions from all reactors.

As the right-hand panel in Figure 1 indicates, the flux of $\bar{\nu}_e$ from the Kashiwazaki complex, producing e^+ with $E_{vis} \sim 4.1 \text{ MeV}$, “falls” in the region of maximum of the survival probability (SPMAX), $P_i(\bar{\nu}_e \rightarrow \bar{\nu}_e) \cong 1$, for both the low-LMA and high-LMA solutions. In contrast, the $\bar{\nu}_e$ with the same energy ($E \sim 3.3 \text{ MeV}$) from the Shika complex located at $\sim 88 \text{ km}$ from KamLAND, are affected by a minimum of the survival probability (SPMIN) in the case of the low-LMA solution, and by a maximum (SPMAX) if the true solution is the high-LMA one. This feature is further illustrated in Figure 2, where we show the positron energy spectrum observed in KamLAND for the two distances of interest - 160 km (Kashiwazaki) and 88 km (Shika). We have plotted the averaged survival probability in each bin for the two solutions. We note that for $L = 160 \text{ km}$, the spectral shape in the statistically important part of the energy spectrum is almost the same for both low-LMA and high-LMA solutions, with SPMAX at about 4 MeV. Since KamLAND receives most of the $\bar{\nu}_e$ flux from the Kashiwazaki complex, this results in the appearance of the two allowed solutions: low-LMA and high-LMA. For a distance of $\sim 88 \text{ km}$ and E_{vis} of about 4.5 MeV, however, the survival probability of interest exhibits a minimum (SPMIN) for the low-LMA solution and a maximum (SPMAX) for the high-LMA one. One could naively expect that a new reactor at the Shika site with a large enough thermal power should make it easier to discriminate between the currently allowed two solutions using the KamLAND data. The presence of the SPMIN for the $\bar{\nu}_e$ flux from Shika in the case of the low-LMA solution might also be expected to improve the precision of the $\sin^2 \theta_\odot$ determination from the KamLAND data¹. Since $P_i(\bar{\nu}_e \rightarrow \bar{\nu}_e)$ has a maximum in the case of the high-LMA solution, one does not expect any improvement in the precision of the $\sin^2 \theta_\odot$ measurement for this solution.

Our preceding discussion was concerned with the signals in KamLAND due to the Kashiwazaki or Shika-2 reactors alone. However, in a realistic evaluation of the physics potential of the KamLAND detector one has to take into account the contributions to the KamLAND signal from all relevant reactors.

III. MEASUREMENT OF THE SOLAR NEUTRINO OSCILLATION PARAMETERS

In this section we generate the prospective KamLAND data with and without the new reactor Shika-2 and study the impact of Shika-2 on the determination of the solar neutrino oscillation parameters using a χ^2 analysis. For the errors we assume a Gaussian distribution and define our χ^2 as

$$\chi^2 = \sum_{i,j} (N_i^{data} - N_i^{theory})(\sigma_{ij}^2)^{-1}(N_j^{data} - N_j^{theory}), \quad (4)$$

where N_i^α ($\alpha = data, theory$) is the number of events in the i^{th} bin and the sum is over all bins. We assume that KamLAND will continue to present their data in 13 bins of width 0.425 MeV with an energy threshold of 2.6 MeV. The error correlation matrix σ_{ij}^2 contains the statistical and systematic errors. While in their first paper the KamLAND collaboration quote a very conservative 6.42% for their systematic error, the latter is expected to diminish with time. The most important contribution to the KamLAND systematic error comes from the uncertainty in the knowledge of the fiducial volume of the detector, which is expected to be reduced. The understanding of the other systematics would reduce the error further. In our analysis we will assume a future KamLAND plausible systematic error of 5%.

In Figure 3 we present the allowed regions in the $\Delta m_\odot^2 - \sin^2 \theta_\odot$ plane, obtained when the spectrum measured by KamLAND is simulated at the low-LMA solution best-fit point (upper panels) and a high-LMA solution point (lower panels). The left panels show the allowed regions obtained with the current set-up of reactors in Japan, with data foreseen to be collected roughly up to March 2006. This corresponds to a statistics of 1.296 kTy. The right panels give the corresponding allowed regions obtained for identical statistics but with the contribution from the future Shika-2 reactor included. We see that with the current reactor set-up in Japan, even the KamLAND data corresponding to

¹ In [24] it was argued that a baseline of 70 km was ideal for the $\sin^2 \theta_\odot$ sensitivity. The Shika distance is close to this best baseline.

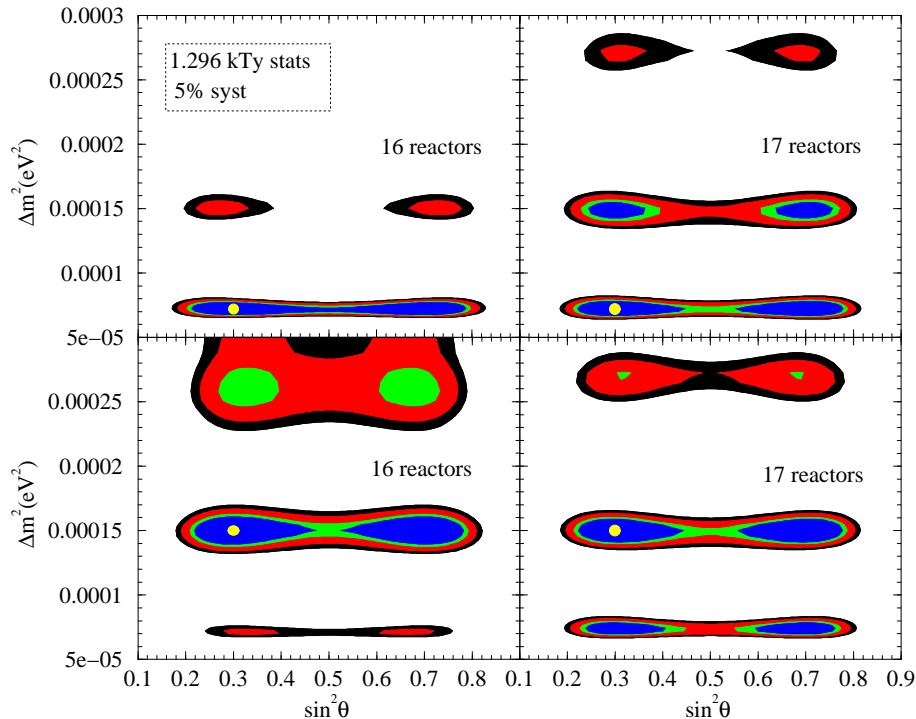


FIG. 3: Prospective 90%, 95%, 99% and 99.73% C.L. contours in the $\Delta m_{\odot}^2 - \sin^2 \theta_{\odot}$ plane, which would be obtained using the KamLAND data corresponding to 1.296 kTy. In the left-hand panels we present results derived with flux from the currently operating 16 reactors, giving the dominant contribution to the signal in KamLAND. The right-hand panels show the corresponding results with the contribution from the Shika-2 reactor added to that of the indicated 16 reactors. The upper(lower) panels in both cases give the allowed regions when low-LMA (high-LMA) is the correct solution. The points at which the spectrum was simulated are shown by yellow circles.

1.296 kTy would still allow the high-LMA (low-LMA) solution at 99% C.L. if the low-LMA (high-LMA) is the true solution. Moreover, if the high-LMA is the correct solution, there would be additional multiple allowed regions at higher values of Δm_{\odot}^2 . Including the contribution from the Shika-2 reactor along with that from the other reactors, makes the ambiguity worse. With the low-LMA (high-LMA) as the true solution, the spurious high-LMA (low-LMA) regions get allowed even at 90% C.L.. There also appears an additional high-LMA solution at $\Delta m_{\odot}^2 \sim 2.6 \times 10^{-4} \text{ eV}^2$. Figure 4 shows the corresponding allowed regions with KamLAND data of 3 kTy. While with 3 kTy of data the KamLAND experiment could determine the correct solution unambiguously with the current set-up of contributing reactors, the presence of the signal from the Shika-2 reactor would make both the low-LMA and high-LMA solutions allowed at 90% C.L. and thus would not permit to resolve the solution ambiguity.

In Figure 5 we show the ratio of the total number of events expected in KamLAND in the case of $\bar{\nu}_e$ oscillations to the corresponding number predicted in absence of oscillations. In this figure we take into account the contributions to the KamLAND event rate from all reactors. This is to be compared with Figure 2 which shows the survival probability expected for the Kashiwazaki and Shika-2 power plants alone. The left panel of Figure 5 shows the ratios for the case with (17 reactors) and without (16 reactors) the contribution of Shika-2 reactor, for the spectrum generated at the low-LMA solution best fit point. The right panel show the corresponding ratio for the data generated at the high-LMA solution best-fit point.

For the low-LMA solution, we had seen from Figure 2 that the signal due to the Kashiwazaki $\bar{\nu}_e$ flux is affected by a SPMAX, while the event rate due to the $\bar{\nu}_e$ from Shika-2 reactor is affected by a SPMIN. The KamLAND detector measures the power weighted cumulative $\bar{\nu}_e$ flux from all reactors. If we consider the effective flux at KamLAND from the i^{th} reactor plant without taking into account the $\bar{\nu}_e$ oscillations,

$$\Phi_{KL}^i = \frac{P_i}{4\pi L_i} \quad (5)$$

we find that for the Kashiwazaki complex it corresponds to $\Phi_{KL} \approx 7.3 \mu\text{W}/\text{cm}^2$, while for the Shika-2 reactor it is sub-

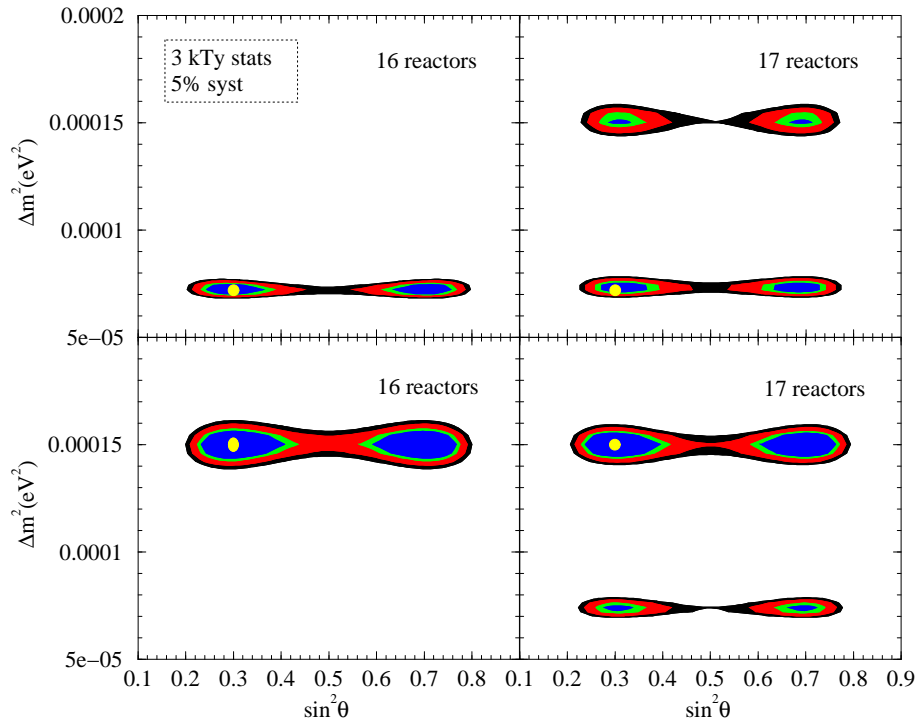


FIG. 4: Same as in Figure 3, but for the larger statistics of 3 kTy.

stantially smaller, $\Phi_{KL} \approx 4.1 \mu W/cm^2$. Thus, the impact on the KamLAND observed signal due to the Kashiwazaki $\bar{\nu}_e$ flux will be considerably larger than that due to the Shika-2 flux, when the contributions from all the reactors are combined. Hence, for the low-LMA solution, the result of adding of the Shika-2 signal on the observed to expected events ratio, is only to decrease it somewhat from that obtained without Shika-2. In other words, even though the oscillations generate big spectral distortions in the spectra of $\bar{\nu}_e$ produced at Kashiwazaki and at Shika-2 reactors, which are reflected in the corresponding e^+ spectra measured by the KamLAND experiment, since the distortion thus produced have opposite effects (corresponding to SPMAX and SPMIN respectively), the net spectral distortion observed in KamLAND would be smaller than in the case of no Shika-2 contribution. This results in increased ambiguity in the determination of Δm_{\odot}^2 , which depends strongly on the magnitude of the distortion in the measured resultant spectrum. This can be seen in the left panel of Figure 5. For the high-LMA solution, both Kashiwazaki and Shika-2 contributions to the spectrum measured at KamLAND are affected by a SPMAX. This results in a mild increase of the spectral distortion for the high-LMA solution with the introduction of Shika-2 signal. Most importantly, as this Figure indicates, after turning on the Shika-2 reactor, the differences between the predicted spectral shapes in the cases of the low-LMA and the high-LMA solution diminish. This explains the increase in the degeneracy between the two solutions, as observed in Figure 3. This degeneracy is not lifted even when statistics is increased to 3 kTy, as seen in Figure 4.

Up to now we have been discussing a scenario where we either have 16 reactors without Shika-2 or we have 17 reactors with Shika-2. The more realistic scenario will be the one where KamLAND collects data with the present 16 reactors until Shika-2 starts operation and thereafter KamLAND will observe the flux from all 17 reactors. It is expected that Shika-2 would begin to operate in March 2006. This implies that KamLAND would have already collected 4 years of data corresponding to 1.296 kTy statistics with the current fiducial volume. In Figure 6 we present the allowed regions of values of Δm_{\odot}^2 and $\sin^2 \theta_{\odot}$ in this more realistic scenario. We consider an aggregate KamLAND statistics of 1.296 kTy with the current 16 reactors and a further 1.296 kTy data with 17 reactors including Shika-2. We assume the same systematic uncertainty of 5% for both the data sets. The Figure shows that with such a combined data set the ambiguity between the low-LMA and high-LMA solutions appears only at 99% C.L., as in the case with just the 16 reactors. It should be noted, however, that even with a total of $2 \times 1.296 \approx 2.6$ kTy data, KamLAND still would not be able to resolve the ambiguity between the two solutions. This should be compared with the 3 kTy results for the 16 reactor set-up given in Figure 4, which show that the ambiguity between the two solutions could be resolved even at the 3σ level. Thus, contrary to what one might naively expect, the advent on Shika-2 will

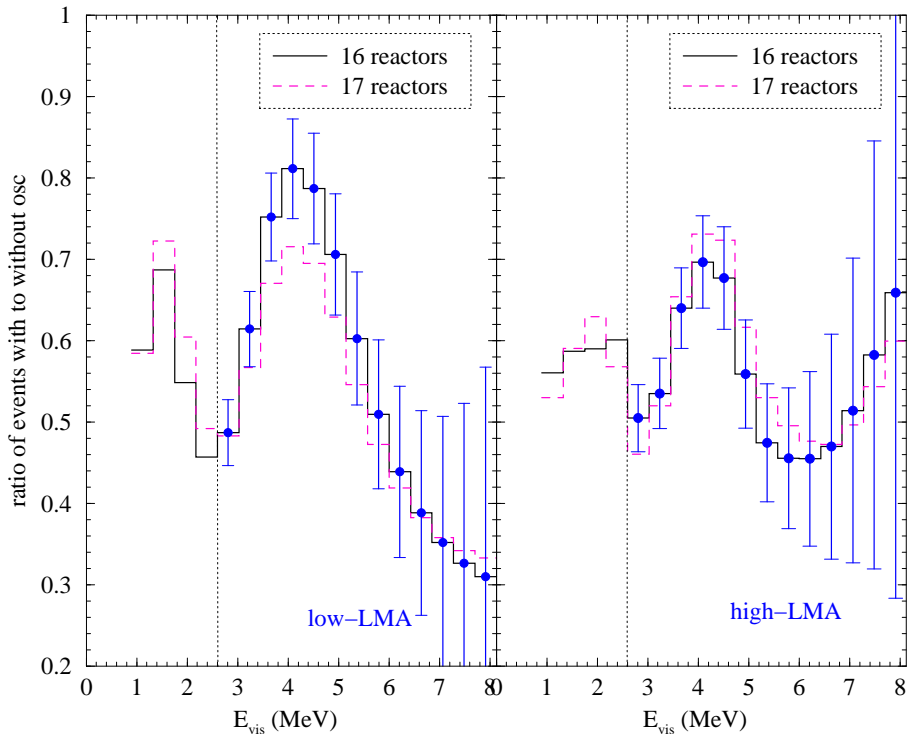


FIG. 5: Expected cumulative positron energy spectral distortion in KamLAND for the low-LMA (left-hand panel) and high-LMA (right-hand panel) solutions. The solid lines display the distortion expected from the present 16 reactor set-up, while the dashed lines give the distortion expected with the Shika-2 reactor contribution included. The error bars show the statistical errors for a KamLAND exposure of 3 kTy and with 16 reactor set-up.

reduce the sensitivity of KamLAND to Δm_{21}^2 .

Next we focus on the impact of the new Shika-2 reactor on the precision of the measurement of $\sin^2 \theta_{\odot}$. From the Figures 3, 4 and 6 we find that there is hardly any improvement in the precision of $\sin^2 \theta_{\odot}$ determination with the inclusion of Shika-2 contribution, contrary to what might be expected. In Table I we present the 99% C.L. allowed ranges of values of $\sin^2 \theta_{\odot}$. The allowed range of $\sin^2 \theta_{\odot}$ for the low-LMA solution diminishes only marginally with the inclusion of the Shika-2 contribution, owing to the effect of the SPMIN, as discussed in [24]. Only the case with 17 reactors and 3 kTy statistics shows some improvement over the 16 reactor case. The improvement here is much less than that obtained in [24] for two major reasons. Firstly, Shika-2 has a thermal power of only 3.926 GW while the reactor considered in [24] had power of 24.3 GW, a la Kashiwazaki. Secondly, in [24] the effect of the presence of other more powerful reactors apart from the reactor producing the SPMIN, was not taken into account. The presence of the other powerful reactors at different baselines (Kashiwazaki, in particular) changes the shape of the resultant positron spectrum at KamLAND from one corresponding to a SPMIN to one corresponding to a SPMAX, as can be seen in Figure 5.

We consider next the hypothetical case of the Kashiwazaki complex operating with reduced power, which would make the SPMIN associated with the Shika-2 contribution more pronounced. The corresponding results are presented in Figure 7. This figure is obtained supposing that KamLAND receives flux from the current 16 reactors, including the Kashiwazaki reactors running at full power up to March 2006 and that thereafter it receives flux from Shika-2 power plant as well for another period of 4 years, giving a total statistics of $1.296 + 1.296$ kTy for the two phases combined. For the second phase, however, we assume that the power of the Kashiwazaki reactor complex is reduced by (i) 50%, and (ii) 100%, i.e., a total shut-down of the Kashiwazaki reactors. The impact on the determination of the solar neutrino oscillation parameters in the former case is shown in the upper panels of Figure 7, while the results for the latter case are displayed in the lower panels of Figure 7. We note that in neither case one can discriminate between the low- and high- LMA solutions and/or can obtain better constraints on $\sin^2 \theta_{\odot}$. In fact, the precision gets worse, owing mainly to the fact that the statistics of the KamLAND experiment decreases significantly if the $\bar{\nu}_e$ flux from the Kashiwazaki complex is cut down.

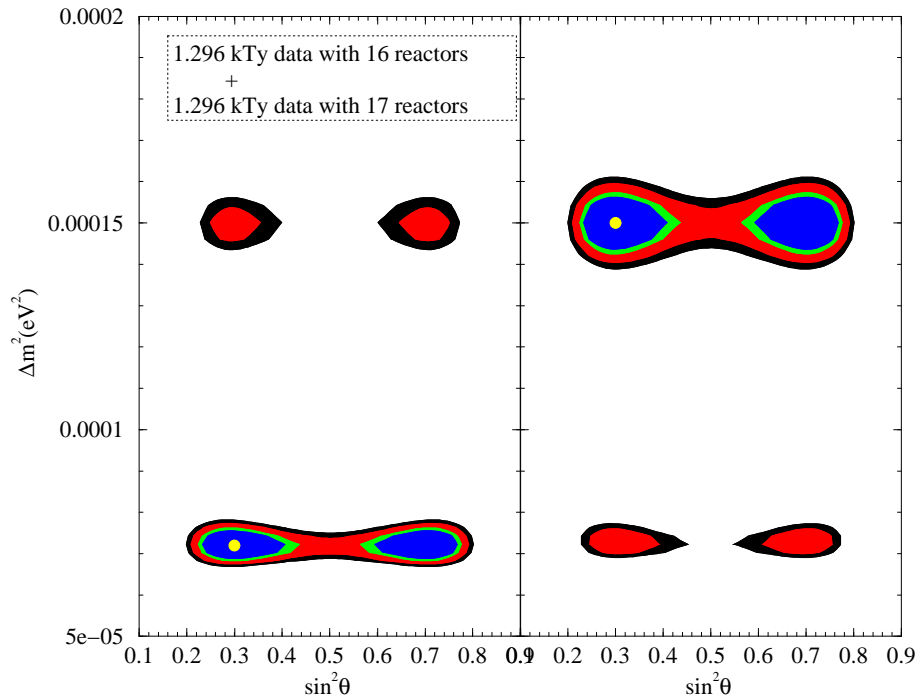


FIG. 6: The C.L. contours obtained from a combined analysis of 1.296 kTy of data collected with 16 reactors as $\bar{\nu}_e$ sources, and an additional 1.296 kTy of data collected when 17 reactors including Shika-2 contribute to the signal in the KamLAND experiment.

Reactor set-up	true solution	Statistics	99% C.L. range for $\sin^2 \theta_\odot$
16	low-LMA	1.296 kTy	0.18 – 0.81
16	high-LMA	1.296 kTy	0.19 – 0.81
17	low-LMA	1.296 kTy	0.19 – 0.80
17	high-LMA	1.296kTy	0.19 – 0.80
16	low-LMA	3.0 kTy	0.21 – 0.45
16	high-LMA	3.0 kTy	0.21 – 0.79
17	low-LMA	3.0 kTy	0.24 – 0.46
17	high-LMA	3.0 kTy	0.21 – 0.78
16+17	low-LMA	1.296 kTy + 1.296 kTy	0.21 – 0.79

TABLE I: The 99% C.L. allowed range of $\sin^2 \theta_\odot$ expected from future data. The first column gives the number of main reactors acting as $\bar{\nu}_e$ source for KamLAND. The final column gives the 99% C.L. range of allowed values of $\sin^2 \theta_\odot$ for the different data sets.

Finally, we present the constraints obtained on Δm_\odot^2 and $\sin^2 \theta_\odot$ when the data from the KamLAND experiment is combined with the global solar neutrino data. In Figure 8 we show the allowed regions derived by combining the global solar neutrino data (including the latest salt phase data from SNO) with the combined 1.296 kTy KamLAND data collected with 16 reactors and 1.296 kTy KamLAND data obtained with 17 reactors, including the Shika-2 flux. A comparison of Figure 6 with Figure 8 shows that the inclusion of the solar neutrino data rules out the spurious high-LMA solution if low-LMA is the correct one. However, if the positron spectrum measured at KamLAND would correspond to a Δm_\odot^2 in the high-LMA region, the solar neutrino data would further increase the degeneracy and make the low-LMA solution allowed at 90% C.L.. In fact, the best-fit Δm_\odot^2 and $\sin^2 \theta_\odot$ for the combined analysis

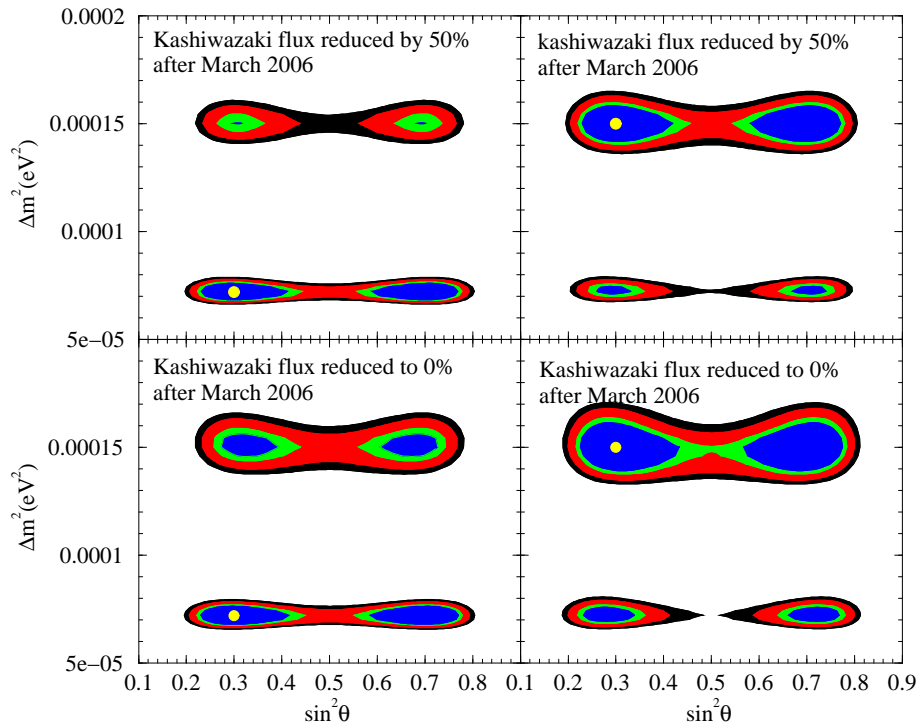


FIG. 7: Same as in Figure 6, but with the Kashiwazaki power reduced by 50% (upper panels) and kashiwazaki power switched off completely (lower panels) after March 2006, when Shika-2 reactor would start operation.

come in the low-LMA zone. The reason for this behavior can be traced to the fact that the solar neutrino data in general, and the SNO data in particular, favor the low-LMA solution over the high-LMA one.

IV. CONCLUSIONS

In the present article we have studied the impact of the $\bar{\nu}_e$ flux from a new reactor, Shika-2, on the sensitivity of the KamLAND experiment to the solar neutrino oscillation parameters, Δm_{\odot}^2 and $\sin^2 \theta_{\odot}$. This upcoming reactor is proposed to have a thermal power of 3.926 GW and would be located at a distance of about 88 km from the KamLAND detector. Since the distance of 88 km corresponds to a minimum (SPMIN) in the resultant positron spectrum at KamLAND, it was expected that the introduction of this detector may improve the precision with which the mixing angle $\sin^2 \theta_{\odot}$ can be determined. However, it follows from our study that the precision of the measurement of the solar neutrino mixing angle, θ_{\odot} , is unlikely to be improved by the addition of this new reactor because of the averaging effect of fluxes from the other reactors. In fact, once the contribution of Shika-2 to the KamLAND event rate is taken into account, the precision to Δm_{\odot}^2 from the KamLAND experiment worsens, increasing the ambiguity between the low-LMA and high-LMA solutions. For the most realistic case where we include the effect of Shika-2 after March 2006 and consider about 2.6 kTy statistics in the simulated KamLAND spectrum, we find that the degeneracy between the two solutions remain at 99% C.L. from the KamLAND data alone, irrespective of whether the KamLAND spectral data is simulated in the low-LMA or high-LMA solution region. We have also presented results on prospective determination of Δm_{\odot}^2 and $\sin^2 \theta_{\odot}$ from the combined KamLAND and the solar neutrino data, including the just published salt phase data from the SNO experiment. Since the SNO salt data disfavors the higher Δm_{\odot}^2 regions, the high-LMA solution is found to be absent if the KamLAND spectrum is simulated in the low-LMA zone. However, if the observed KamLAND spectrum corresponds to oscillation parameters in the high-LMA zone, the ambiguity between the low-LMA and high-LMA solutions would remain as a result of the conflicting trends of the KamLAND and the current solar neutrino data.

Acknowledgements.

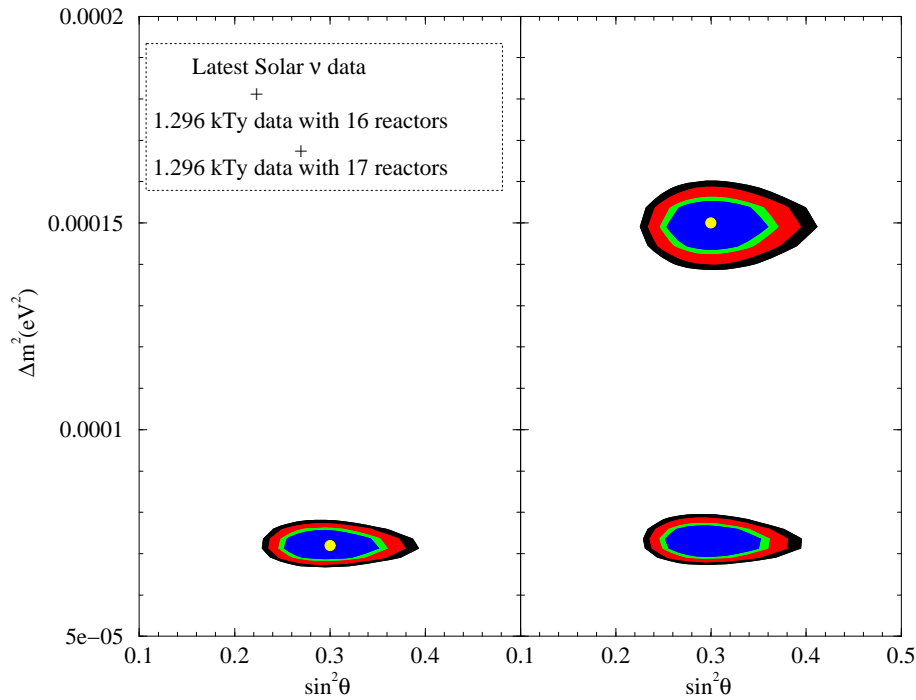


FIG. 8: The combined allowed C.L. contours expected after combining the global solar neutrino data, including the salt enriched SNO results, with the total data obtained from KamLAND after 1.296 kTy data with 16 reactors and 1.296 kTy data with the 17 reactors including Shika-2. The left-hand panel corresponds to low-LMA as true solution while the right-hand panel gives the allowed areas obtained if high-LMA was true.

We would like to thank F. Suekane for useful correspondence. S.T.P. acknowledges informative discussions with K. Heeger. This work was supported in part by the Italian MIUR and INFN under the programs “Fenomenologia delle Interazioni Fondamentali” (S.T.P. and S.G.) and “Fisica Astroparticellare” (S.C.).

-
- [1] B.T. Cleveland *et al.*, *Astrophys. J.* **496** (1998) 505; Y. Fukuda *et al.*, *Phys. Rev. Lett.* **77** (1996) 1683; V. Gavrin, *Nucl. Phys. Proc. Suppl.* **91** (2001) 36; W. Hampel *et al.*, *Phys. Lett.* **B447** (1999) 127; M. Altmann *et al.*, *Phys. Lett.* **B490** (2000) 16.
- [2] Super-Kamiokande Coll., Y. Fukuda *et al.*, *Phys. Rev. Lett.* **86** (2001) 5656 and 5651.
- [3] SNO Coll., Q.R. Ahmad *et al.*, *Phys. Rev. Lett.* **87** (2001) 071301.
- [4] SNO Coll., Q.R. Ahmad *et al.*, *Phys. Rev. Lett.* **89** (2002) 011302 and 011301.
- [5] KamLAND Coll., K. Eguchi *et al.*, *Phys. Rev. Lett.* **90** (2003) 021802.
- [6] S.T. Petcov, Lecture Notes in Physics, v. **512** (eds. H. Gausterer and C.B. Lang, Springer, 1998), p. 281 (arXiv:hep-ph/9806466); S. Goswami, *Pramana* **60**, 261 (2003), (arXiv:hep-ph/0305111); M.C. Gonzalez-Garcia and Y. Nir, *Rev. Mod. Phys.* **75** (2003) 345.
- [7] C.-S. Lim and W. Marciano, *Phys. Rev.* **D37** (1988) 1368; E.Kh. Akhmedov, *Phys. Lett.* **B213** (1988) 64.
- [8] M.M. Guzzo, A. Masiero and S.T. Petcov, *Phys. Lett.* **B260** (1991) 154; E. Roulet, *Phys. Rev.* **D44** (1991) R935.
- [9] M. Gasperini, *Phys. Rev.* **D39** (1989) 3606; A. Halprin and C.N. Leung, *Phys. Rev. Lett.* **67** (1991) 1833; S. Coleman and S. Glashow, *Phys. Lett.* **B405** (1997) 249.
- [10] B. Pontecorvo, Chalk River Lab. report PD-205, 1946; *Zh. Eksp. Teor. Fiz.* **53** (1967) 1717.
- [11] R. Davis, D.S. Harmer and K.C. Hoffman, *Phys. Rev. Lett.* **20**, 1205 (1968); *Acta Physica Acad. Sci. Hung.* **29** Suppl. 4, 371 (1970); R. Davis, Proc. of the “Neutrino ‘72” Int. Conference, Balatonfured, Hungary, June 1972 (eds. A. Frenkel and G. Marx, OMKDK-TECHNOINFORM, Budapest, 1972), p. 5.
- [12] A. Bandyopadhyay, S. Choubey, R. Gandhi, S. Goswami and D. P. Roy, *Phys. Lett. B* **559**, 121 (2003) [arXiv:hep-ph/0212146];
- [13] G. L. Fogli *et al.*, *Phys. Rev. D* **67**, 073002 (2003) [arXiv:hep-ph/0212127]; M. Maltoni, T. Schwetz and J. W. Valle, arXiv:hep-ph/0212129; J. N. Bahcall, M. C. Gonzalez-Garcia and C. Pena-Garay, *JHEP* **0302**, 009 (2003) [arXiv:hep-ph/0212147]; H. Nunokawa, W. J. Teves and R. Zukanovich Funchal, arXiv:hep-ph/0212202; P. Aliani *et al.*,

- arXiv:hep-ph/0212212; P. C. de Holanda and A. Y. Smirnov, JCAP **0302**, 001 (2003) [arXiv:hep-ph/0212270].
- [14] SNO Coll., S.N. Ahmed et al., arXiv:nucl-ex/0309004.
 - [15] M. Maris and S. T. Petcov, Phys. Lett. B **534**, 17 (2002) [arXiv:hep-ph/0201087].
 - [16] A. Bandyopadhyay, S. Choubey, S. Goswami, S.T. Petcov and D. P. Roy, hep-ph/0309174.
 - [17] M. Maltoni, T. Schwetz, M. A. Tortola and J. W. Valle, arXiv:hep-ph/0309130. P. Aliani, V. Antonelli, M. Picariello and E. Torr ente-Lujan, arXiv:hep-ph/0309156.
 - [18] Y. Fukuda *et al.* [Super-Kamiokande Collaboration], Phys. Rev. Lett. **81**, 1562 (1998) [arXiv:hep-ex/9807003]; M. Shiozawa, talk given at the Int. Conf. on Neutrino Physics and Astrophysics “Neutrino’02”, May 25 - 30, 2002, Munich, Germany.
 - [19] Super-Kamiokande Coll., Y. Hayato *et al.*, Talk given at the Int. EPS Conference on High Energy Physics, July 17 - 23, 2003, Aachen, Germany.
 - [20] S.T. Petcov, Invited talk given at the First Yamada Symposium on Neutrinos and Dark Matter in Nuclear Physics, June 9 - 14, 2003, Nara, Japan, Ref. SISSA 72/03/EP (<http://ndm03.phys.sci.osaka-u.ac.jp>).
 - [21] M. Maris and S. T. Petcov, Phys. Rev. D **62**, 093006 (2000) [arXiv:hep-ph/0003301].
 - [22] A. Bandyopadhyay, S. Choubey, R. Gandhi, S. Goswami and D. P. Roy, arXiv:hep-ph/0211266.
 - [23] V. D. Barger, D. Marfatia and B. P. Wood, Phys. Lett. B **498**, 53 (2001) [arXiv:hep-ph/0011251]; H. Murayama and A. Pierce, Phys. Rev. D **65**, 013012 (2002) [arXiv:hep-ph/0012075]; A. de Gouvea and C. Pena-Garay, Phys. Rev. D **64**, 113011 (2001) [arXiv:hep-ph/0107186].
 - [24] A. Bandyopadhyay, S. Choubey and S. Goswami, Phys. Rev. D **67**, 113011 (2003) [arXiv:hep-ph/0302243].
 - [25] J. N. Bahcall and C. Pena-Garay, arXiv:hep-ph/0305159.
 - [26] S. T. Petcov and M. Piai, Phys. Lett. B **533**, 94 (2002) [arXiv:hep-ph/0112074].
 - [27] S. Choubey, S. T. Petcov and M. Piai, arXiv:hep-ph/0306017.
 - [28] K. Nakamura, Talk at the 5th International Workshop on Neutrino Factories & Superbeams (NuFact’03), Columbia University, New York, June 5-11, 2003; <http://www.cap.bnl.gov/nufact03/>